Direct and indirect detection and LHC signals of bino-Higgsino dark matter

Ilia Gogoladze, Rizwan Khalid, Yukihiro Mimura, and Qaisar Shafi

Direct and Indirect Detection and LHC Signals of Bino-Higgsino Dark Matter

Ilia Gogoladze[a1], Rizwan Khalid[a2], Yukihiro Mimura[a,b], and Qaisar Shafi[a]

[a] *Bartol Research Institute, Department of Physics and Astronomy,*
University of Delaware, Newark, DE 19716, USA
[b] *Department of Physics, National Taiwan University, Taipei, Taiwan 10617, R.O.C.*

Abstract

If the lightest dark matter neutralino has a sufficiently large Higgsino component, its spin-independent and spin-dependent cross sections on nucleons can be sizable enough to be detected soon in direct and indirect surveys. We outline in this paper some characteristic features expected of mixed bino-Higgsino dark matter. If the observed relic density is saturated by the bino-Higgsino dark matter, it fixes the amount of allowable bino-Higgsino mixing and provides predictions for other observables which can be tested at the Large Hadron Collider (LHC). We study the correlation between the cross sections and the branching ratio of $B_s \to \mu^+\mu^-$. For a mixed bino-Higgsino dark matter, the mass differences of the neutralinos can be less than M_Z. This will cause an excess of lepton pairs, above the Standard Model predictions, from the decays of the two heavier neutralinos. We discuss implications of the dilepton invariant mass distribution, and outline a way to extract the neutralino parameters for testing gaugino mass unification and deducing the relic density from an interplay of astrophysical detection and LHC measurements.

---

[1] Email: ilia@bartol.udel.edu. On leave of absence from: Andronikashvili Institute of Physics, GAS, Tbilisi, Georgia.
[2] Email: rizwan.hep@gmail.com. On study leave from: Centre for Advanced Mathematics & Physics of the National University of Sciences & Technology, H-12, Islamabad, Pakistan.

1 Introduction

There exists overwhelming evidence, most recently from the Wilkinson Microwave Anisotropy Probe (WMAP) [1], that non-baryonic cold dark matter comprises around 23 percent of the Universe's energy density. Identifying this dark matter, presumably an elementary particle, is one of the foremost contemporary challenges in particle physics and cosmology. The goals for successful identification of dark matter are: (1) Detection of the relic dark matter particle, and measurement of its mass and distribution directly. (2) Production of the dark matter particle at the LHC and future linear colliders, and measurement of its properties. (3) Testing the consistency between these measurements, namely in astrophysics and particle physics, and reproduction of the relic abundance of the particle from the measured properties in order to confirm that the dark matter particle (possibly more than one species of particles) really makes up 23 percent of the Universe's energy density.

One of the most compelling features of low scale supersymmetry (SUSY), supplemented with R-parity conservation, is that it can provide an attractive cold dark matter candidate with the correct relic abundance, provided the lightest neutralino $\tilde{\chi}_1$ is also the lightest SUSY particle (LSP) [2]. If the LSP neutralino is bino dominated (in an admixture of bino, wino, and Higgsinos), it often leads to an over-abundance of dark matter, unless (co)annihilation processes reduce the relic density to levels compatible with WMAP. Many solutions have been proposed to accomplish this [2, 3].

One attractive scenario for realizing the correct relic abundance is to consider an appropriate bino-Higgsino mixture in the composition of the LSP [4, 5, 6]. In this mixed bino-Higgsino LSP (called bino-Higgsino dark matter) scenario, which is realized in so called Hyperbolic Branch/Forcus Point [7, 8] in the minimal supergravity model, two neutralinos and one chargino have masses that are close to the LSP mass, such that (co)annihilation processes among them can reproduce the desired relic density. The spin-independent (SI) cross section on nuclei in this scenario is enhanced, which is an advantage from the point of view of direct detection experiments searching for the LSP. Indeed, the recent candidate events reported by CDMSII [9] and EDELWEISS-II [10] would suggest that the SI cross section is $O(10^{-8})$ pb. This is of the right order of magnitude for the bino-Higgsino dark matter scenario [11, 12]. As the bounds on the cross section get lowered by the ongoing and planned measurements by XENON100 [13], SuperCDMS [14], and XMASS [15], the WMAP compatible bino-Higgsino mixing solutions will be among the first ones to be tested. Moreover, it is known that a significant Higgsino component in the LSP neutralino also gives a large spin-dependent (SD) cross section, which would make the indirect detection of this dark matter through self-annihilation into neutrinos and other particles more feasible. Thus, the bino-Higgsino dark matter solution will be tested

by the IceCube/Deep Core neutrino observatory [17]. It is important to observe both SI and SD cross sections and to see their correlation [18] in order to adequately test the bino-Higgsino dark matter scenario.

The SI cross section is enhanced if the mass m_A of the CP-odd Higgs boson is small and $\tan\beta$ (ratio of Higgs vacuum expectation values (VEVs)) is large. With m_A small, pair annihilation processes are enhanced, and a reduced bino-Higgsino mixing can give rise to the desired WMAP relic density. We refer to this case as bino-Higgsino-like dark matter, if we need to distinguish among the WMAP solutions. On the other hand, when we specify a mixed bino-Higgsino LSP solution where (co)annihilation processes via scalars are negligible, we refer to it as well-tempered bino-Higgsino dark matter [5]. From the particle physics point of view, the rare decay $B_s \to \mu^+\mu^-$ is one of the most interesting processes in the region of large $\tan\beta$ and small m_A [19]. The Tevatron will provide a bound ($\sim 2 \times 10^{-8}$) on this branching ratio in run II [20], and LHCb, within a few years, will probe the standard model prediction $(3 - 4) \times 10^{-9}$. (The exclusion limit from 1 fb^{-1} of data expected by the end of 2011 will be $\sim 6 \times 10^{-9}$) [21]. It is thus important to investigate the regions of parameter space that provide larger SI cross sections (small m_A and/or small Higgsino mass μ), and to explore their predictions.

At the LHC, the neutralino LSP is created from cascade decays of squarks and gluinos, and manifests itself as missing energy. As mentioned above, to identify dark matter, one major goal is to reproduce the LSP relic density from the collider measurements [22]. However, the inverse problem at the LHC [23] is not so easy in general, since it is hard to measure the mass spectrum and the couplings directly. Several techniques have been developed, and several reliable relic density simulations have been explored for various WMAP solutions [24, 25, 26, 27]. The assumptions of universality and/or unification of the SUSY breaking mass parameters are crucial simplifications for the collider measurements of the relic density. For the bino-Higgsino dark matter, universality of the sfermion masses is less important since, by definition, the coannihilation processes via sfermions are negligible as far as the relic density is concerned. The gaugino mass spectrum (which should also be addressed at the LHC [28]) will be more important in restricting the relic density with LHC measurements.

In this paper we investigate bino-Higgsino dark matter and its implications for direct and indirect detection, and for the LHC measurements. We will study both the well-tempered bino-Higgsino dark matter and bino-Higgsino-like dark matter with smaller m_A. In the study of the well-tempered mixing solution, it is assumed that the sfermions are sufficiently heavy, without specifying the SUSY breaking scenario or any underlying theory. This is done in order to make the bino-Higgsino dark matter relic density, and the SI and SD cross sections insensitive to these masses. The bino-Higgsino mixing needed to satisfy the desired WMAP relic density depends

on wino and bino mass ratio, and thus the cross sections implicitly depend on this ratio. For simplicity, we assume gaugino unification at the grand unification scale, M_{GUT}, in order to investigate the cross sections. We also study the possibility of non-universal gauginos, which also can be tested experimentally within our framework. Our results should be applicable to any model where the well-tempered bino-Higgsino dark matter solution can be realized. On the other hand, in order to exhibit our study of the correlation of cross sections and $\mathrm{Br}(B_s \to \mu^+\mu^-)$ for bino-Higgsino-like dark matter, we employ non-universal Higgs mass boundary conditions, where m_A and μ are free low energy parameters. In this case, for a given LSP mass and m_A, the proper WMAP relic density constrains the Higgsino mass μ. As a result, the chargino contribution to $\mathrm{Br}(B_s \to \mu^+\mu^-)$ is predictable for a given stop mass, if gaugino mass unification is assumed.

In our presentation we first study the constraints and implications from SI and SD cross sections for the bino-Higgsino(-like) dark matter solution. If the SI cross section is large ($\sigma_{\mathrm{SI}} \gtrsim 10^{-8}$ pb), the bino-Higgsino mixing is large and/or m_A is small. The SD cross section is restricted, for given m_A if the bino-Higgsino mixing is determined by the WMAP observation. If the CP-odd Higgs mass m_A is small, the amount of bino-Higgsino mixing required to satisfy the WMAP relic density is not very large. The SD cross section, accordingly, is then also not very large. Hence it is worth making clear the conditions under which we can observe the SD cross section by indirect detection, as well as the corresponding prediction for $\mathrm{Br}(B_s \to \mu^+\mu^-)$, while satisfying the other experimental constraints. When m_A is large, the bino-Higgsino mixing needs to be well-tempered and the SD cross section must be large. We also investigate the bound on SD cross section for smaller neutralino masses, $\lesssim 100$ GeV, since it is already bounded by the recent CDMSII / XENON100 data.

We then proceed to study the implication from LHC measurements. If the bino-Higgsino mixing is well-tempered, three of the mass eigenvalues of the neutralino mass matrix can be degenerate to within $O(M_Z)$, depending on the neutralino mass parameters. In such a case, the dilepton invariant mass distribution from the heavier neutralino decay with missing energy will give us important information on the neutralino mass parameters. Due to the large SI cross section, the mass of the bino-Higgsino dark matter particle is expected to be measured from the distribution of the recoil energy of the heavy nuclei in the direct detection experiments, and there arises a possibility to extract the parameters for reproducing the LSP relic density and the gaugino mass spectrum.

This article is organized as follows. In Section 2, the SI and SD cross sections of neutralino-nucleon interactions are briefly studied. In Section 3, the correlation between the bino-Higgsino dark matter solution and SI cross section is described. Within the bino-Higgsino dark matter

scenario, the interplay between the SD cross section and $\mathrm{Br}(B_s \to \mu^+ \mu^-)$ is presented in Section 4. We discuss in Section 5 several possible signatures of this scenario at the LHC, and in Section 6 we summarize our results.

2 Spin-Independent and Spin-Dependent Cross Sections

The Higgs exchange diagrams dominate the SI cross section of the lightest neutralino on nucleon [2, 29] as long as squarks are sufficiently heavy. Also, for $m_H \lesssim m_h \sqrt{\tan\beta}$, the contribution from the heavier Higgs (H) exchange is dominant over the lighter Higgs (h). The SI cross section in this case can be written as

$$\sigma_{\mathrm{SI}} \simeq \frac{m_N^4}{4\pi} \frac{g_2^4}{M_W^2} \frac{\cos^2\alpha}{\cos^2\beta} \frac{F_H^2}{m_H^4} \left[(f_d + f_s + \frac{2}{27}f_G) + \frac{\tan\alpha}{\tan\beta}(f_u + \frac{4}{27}f_G) \right]^2, \tag{1}$$

where α is the Higgs mixing angle, $\tan\beta \equiv \langle H_2 \rangle / \langle H_1 \rangle$ is the ratio of up- and down-type Higgs VEVs, M_W is the W boson mass, g_2 is the $SU(2)$ gauge coupling, m_N is the nucleon mass, $f_q = m_q \langle N|\bar{q}q|N\rangle/m_N$ for nucleon N, $f_G = 1 - f_u - f_d - f_s$, and $F_H = (N_{12} - N_{11}\tan\theta_W)(N_{14}\sin\alpha - N_{13}\cos\alpha)$. N_{1i} are the elements of the diagonalizing matrix of the neutralino mass matrix such that the lightest neutralino can be written as a linear combination of gauginos and Higgsinos:

$$\tilde{\chi}_1 = N_{11}\tilde{B} + N_{12}\tilde{W} + N_{13}\tilde{H}_1 + N_{14}\tilde{H}_2. \tag{2}$$

The lighter Higgs exchange also contributes to the SI cross section which, therefore, does not vanish ($\sim 10^{-8}$ pb) even if $m_A \gtrsim 1$ TeV in the case of bino-Higgsino dark matter ($N_{11}N_{13} \sim 0.1$).

The strange sea quark content of the nucleon is very important from the point of view of computing the SI cross section [30]. Recent lattice collaborations report small values of f_s [31, 32, 33]. The smallest value is reported by the JLQCD collaboration in 2009 as $f_s = 0.02$, with $f_s < 0.08$ to within 1σ. For $f_s = 0.118$ (which is the default value of the numerical package ISAJET [34] that we use), the cross section is roughly a factor 2 larger when compared to the case of small f_s. If we use a larger value of f_s ($\sim 0.2 - 0.4$), the bino-Higgsino dark matter is on the edge of the current bound set by CDMSII and XENON100, and is even excluded in particular for small m_H. We will use the value $f_s = 0.03$ in this paper. For $f_{u,d}$, the default values of ISAJET are used ($f_u = 0.023$, $f_d = 0.034$ for protons).

The SD cross section, σ_{SD}, is dominated by the Z boson exchange diagram [2, 29] provided the squarks are sufficiently heavy,

$$\sigma_{\mathrm{SD}} \propto \frac{1}{M_Z^4}(N_{13}^2 - N_{14}^2)^2. \tag{3}$$

In this case, the SD cross section depends only on neutralino mixing (disregarding hadronic uncertainty), and it thus provides a good probe of the gaugino and Higgsino parameters. Large SD

cross sections clearly prefer a large Higgsino component for the LSP. If the Higgsino component is dominant (which can happen for the lightest neutralino mass $m_{\chi_1} \sim 1$ TeV satisfying the relic abundance), however, the SI and SD cross sections are smaller since $|N_{13}| \simeq |N_{14}| \gg |N_{11}|, |N_{12}|$ is satisfied. If the LSP mass is less than M_Z, the SD cross section is maximized while satisfying the WMAP data. However, if we assume gaugino mass unification, the bino-Higgsino solution with a large SD cross section is excluded by the chargino mass bound $m_{\tilde{\chi}_1^+} \geq 103$ GeV [35].

As the dark matter gets scattered by nucleons in the sun it loses kinetic energy, and eventually will not be able to escape from the sun's gravity. As a result, a larger SD cross section gives rise to a larger population of neutralinos in and around the sun [2]. This population of neutralinos will manifest itself through self-annihilation into high energy neutrinos (or muons) emerging from the sun. High energy neutrinos can be observed if the SD cross section is sufficiently large [37]. The bino-Higgsino mixing solution was explored by AMANDA [16], and it will also be tested by IceCube/Deep Core [17].

3   Bino-Higgsino Dark Matter and SI Cross Section

In the bino-Higgsino dark matter scenario, the SI cross section is almost determined by the parameters m_A and μ for a given LSP mass and $\tan\beta$. For a more general description of this scenario, we consider non-universal Higgs mass boundary conditions so as to keep μ and m_A free. We assume universal trilinear couplings, A_0, as well as universal soft gaugino and sfermion masses $m_{1/2}$ and m_0 respectively. For the purposes of this analysis, the universality of sfermion masses is not crucial, especially for the case of well-tempered bino-Higgsino dark matter.

In Fig. 1 we show contours for Ωh^2 and $\sigma_{\rm SI}$ in the m_A-μ plane for fixed lightest neutralino mass $m_{\tilde{\chi}_1} = 150$ GeV, $\tan\beta = 10, 40$ and $A_0 = 0$. The $\Omega h^2 \sim 0.11$ contour is shown for $m_0 = 500$ GeV (dotted red line) and $m_0 = 2$ TeV (dotted blue line). The SI cross section contours correspond to 1×10^{-9}pb (black line), 1×10^{-8}pb (orange line), 3×10^{-8}pb (purple line) and 4.7×10^{-8}pb (green line). The SI cross section becomes larger for a larger $\tan\beta$. For $m_A = 2m_{\tilde{\chi}_1}$, Ωh^2 is tiny ($\ll 0.1$) due to the s-channel resonance in the pair annihilation processes, and the so called A-funnel WMAP solutions [36] lie near this line. For smaller μ, the second lightest neutralino gets closer in mass to $m_{\tilde{\chi}_1}$ and bino-Higgsino mixing becomes larger. Therefore, the WMAP contour shifts away from the A-resonance solution. For $m_A \lesssim 2m_{\tilde{\chi}_1} - m_h$, the pair annihilation channels $\tilde{\chi}_1\tilde{\chi}_1 \to Hh, ZA$ open up. As a result, the bino-Higgsino mixing should be smaller (μ should be larger) for the left branch of the Ωh^2 solutions, as shown in the figure.

Next let us describe the behavior of sfermion masses in the m_A-μ plane for fixed m_0, $\tan\beta$ and A_0. With smaller μ, the SUSY breaking up-type Higgs mass squared is larger (but not its
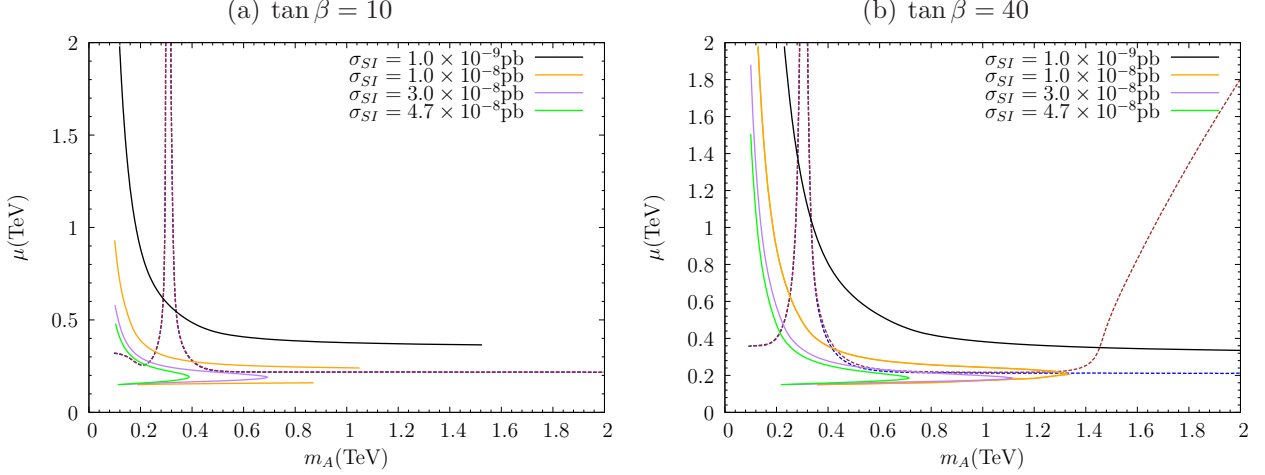
Figure 1: The contours for SI cross section (solid lines) and $\Omega h^2 = 0.11$ (dotted lines) for a fixed lightest neutralino mass $m_{\tilde{\chi}_1} = 150$ GeV and $A_0 = 0$. The left and right panels correspond to $\tan\beta = 10, 40$ respectively. The $\Omega h^2 \sim 0.11$ contour is shown for $m_0 = 500$ GeV (dotted red line) and $m_0 = 2$ TeV (dotted blue line). The SI cross section contours correspond to 1×10^{-9}pb (black line), 1×10^{-8}pb (orange line), 3×10^{-8}pb (purple line) and 4.7×10^{-8}pb (green line, current limit).

absolute value since $m_{H_u}^2 \simeq M_Z^2/2 - \mu^2$). Therefore, the RGE evolution of sfermion masses, which couple to up-type Higgs, drives the masses to smaller values. An exception occurs if Higgsino dominates the lightest neutralino, $\mu \sim m_{\tilde{\chi}_1}$. In this region, M_1 is larger (for fixed $m_{\tilde{\chi}_1}$), and the sfermion masses are also larger due to the wino and gluino loops since gaugino unification is assumed. For larger m_A and/or smaller μ, the SUSY breaking down-type Higgs squared mass is larger because $m_A^2 = 2\mu^2 + m_{H_u}^2 + m_{H_d}^2$ and, thus, $m_{H_d}^2 \simeq m_A^2 - \mu^2 - M_Z^2/2$. The RGE evolution for sfermions masses, which couple to the down-type Higgs, therefore, drives them to smaller values, especially if $\tan\beta$ is large. As a result, for small m_0, the stau-coannihilation region (and also the stau LSP region) appears in the bottom-right corner of Fig. 1, and the Ωh^2 contour is thus lifted up. We comment that stop-coannihilation can happen if A_0 is modified to make the left-right stop mixing to be larger. Furthermore, in the region of small μ, $m_{H_u}^2 > m_{H_d}^2$ is needed at the unification scale. This then forces the sfermions with positive hypercharges to become lighter. In the region of large μ, on the other hand, the sfermions with negative hypercharges become lighter, and thus a sneutrino can be NLSP for large μ and small m_0, such that sneutrino-coannihilation can be realized. Since we are interested in smaller μ values to obtain large cross sections, we do not discuss the coannihilation solutions.

In order to facilitate direct detection and determination of the dark matter mass, we are interested in large SI cross sections $\gtrsim 10^{-8}$ pb. One can see from Fig. 1 that the points that satisfy both the WMAP data and $\sigma_{\rm SI} > 10^{-8}$ pb are separated into two regions because of

7

the A-resonance. One region corresponds to $m_A < 2m_{\tilde{\chi}_1}$ (left branch), while the other to $m_A > 2m_{\tilde{\chi}_1}$ (right branch). The SD cross section is larger for the region $m_A > 2m_{\tilde{\chi}_1}$ because of the larger bino-Higgsino mixing needed to satisfy WMAP data, as previously described. Such large SD cross sections are definitely testable at IceCube/Deep Core [17]. For the $m_A < 2m_{\tilde{\chi}_1}$ region, the SD cross section is correspondingly smaller to satisfy WMAP data. However, in this region, the branching ratio of the decay $B_s \to \mu^+\mu^-$ can be large (for $\tan\beta \gtrsim 30$) as the heavier Higgs can be light and the Higgs penguin contribution is enhanced. The SUSY enhancement of $B_s \to \mu^+\mu^-$ can be tested at the LHC, and it is important to investigate the possible values of the branching ratio. Also, in this region, the SD cross section may be on the verge of being tested by IceCube/Deep Core.

4   Correlation between Cross Sections and $\mathrm{Br}(B_s \to \mu^+\mu^-)$

Since the SI cross section and $\mathrm{Br}(B_s \to \mu^+\mu^-)$ are sensitive to the heavier Higgs mass, a numerical analysis to see the correlation between the two is interesting [38]. If there exists non-minimal flavor violation, the CP violating phase in B_s-$\bar{B}_s$ mixing can also be important [39]. In this section, we will explore the prospects of neutralino detection via the SD cross section inferred from observation of neutrino flux from the sun by IceCube/Deep core observations. We will also discuss the correlation between the SD cross section and the SUSY contribution to $\mathrm{Br}(B_s \to \mu^+\mu^-)$ in the case of minimal flavor violation.

As mentioned in the previous section, we employ non-universal Higgs boundary conditions with universal sfermion masses and gaugino mass unification in order to exhibit our results. Since universality of sfermion masses is not crucial to describe the bino-Higgsino mixing solutions, we do not impose constraints from the slepton mass spectrum (arising from muon $g-2$ for instance). Instead, we employ the constraints from $b \to s\gamma$ to describe the correlation between SI and SD cross sections and $\mathrm{Br}(B_s \to \mu^+\mu^-)$.

If no FCNC source is introduced in the SUSY breaking mass parameters, the important contribution to $\mathrm{Br}(b \to s\gamma)$ comes from the chargino and charged Higgs loops. The chargino contribution to the amplitude for $b \to s\gamma$ transition is (naively) proportional to $\tan\beta$, while the charged Higgs contribution does not depend very much on $\tan\beta$. The latter contribution has a positive sign for the amplitude, while the chargino contribution gives a negative sign for the amplitude when $\mu > 0$. These two contributions can therefore be canceled through an appropriate choice of parameters.

For $m_A > 400 - 500$ GeV (with a slight dependence on $\tan\beta$), the branching fraction $\mathrm{Br}(b \to s\gamma)$ is smaller than $\sim 4.2 \times 10^{-4}$ in the SUSY particle decoupling limit. Therefore, only lower bounds on the SUSY particle masses are obtained in this case. If the Higgsino mass is
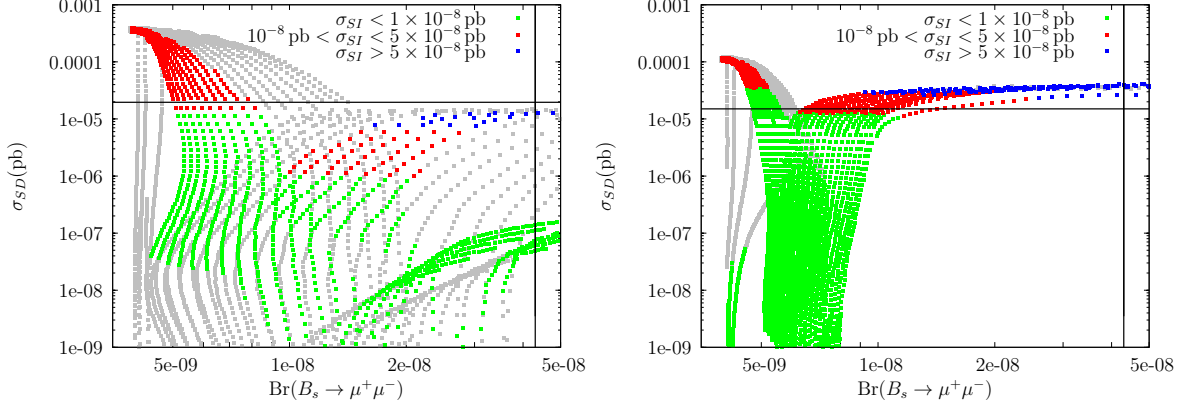
Figure 2: $\mathrm{Br}(B_s \to \mu\mu)$ vs σ_{SD} plots for $\Omega h^2 = 0.11$, $\tan\beta = 40$, $A_0 = 0$, $m_{\tilde{\chi}_1} = 150$ GeV (left), $m_{\tilde{\chi}_1} = 300$ GeV (right). Green points satisfy $\mathrm{Br}(b \to s\gamma)$ and m_h bounds. Red points satisfy the CDMSII bound and $\sigma_{\mathrm{SI}} > 10^{-8}$ pb. Blue points are excluded by the CDMSII bound. The current bound on $\mathrm{Br}(B_s \to \mu^+\mu^-)$ (4.3×10^{-8}) at the 95% confidence level is shown as a vertical line. The horizontal line indicates the expected sensitivity of IceCube/Deep Core.

fixed to obtain the proper relic density for a given LSP mass, the stop mass is bounded from below.

For $m_A < 400 - 500$ GeV, however, the chargino contribution is needed to satisfy the experimental constraint on $\mathrm{Br}(b \to s\gamma)$, and the stop mass is also bounded from above. For small $\tan\beta$, in particular, the LEPII bound $m_h > 114.4$ GeV can be more important than $\mathrm{Br}(b \to s\gamma)$ for the lower bound on the stop mass. As a result, small m_A values can be excluded by a combination of $\mathrm{Br}(b \to s\gamma)$ and m_h bounds.

Fig. 2 shows a plot in $\mathrm{Br}(B_s \to \mu^+\mu^-)$ - σ_{SD} plane for $m_{\tilde{\chi}_1} = 150$ GeV (left panel) and 300 GeV (right panel). The points shown satisfy the WMAP 2σ bounds on Ωh^2 and are generated using $m_0 < 2$ TeV, $0 < \mu < 2$ TeV, $m_A < 2$ TeV, $A_0 = 0$ and $\tan\beta = 40$. In the right branch ($m_A > 2m_{\chi_1}$) of the WMAP solution, m_A is large and thus $\mathrm{Br}(B_s \to \mu^+\mu^-)$ is comparable to the SM prediction. One finds that the SD cross section is large in this branch. The points for the left branch ($m_A < 2m_{\chi_1}$) have $\mathrm{Br}(B_s \to \mu^+\mu^-)$ that is bounded from both above and below. The maximal values of $\mathrm{Br}(B_s \to \mu^+\mu^-)$ and the SD cross section in the left branch have already been excluded by the CDMSII bound.

The SD cross section for the left branch is below the sensitivity of IceCube/Deep core for $m_{\tilde{\chi}_1} = 150$ GeV, but lies on the boundary for $m_{\tilde{\chi}_1} = 300\,\mathrm{GeV}$. Indeed, to observe both a large $\mathrm{Br}(B_s \to \mu^+\mu^-)$, enhanced by sufficiently small m_A, and a large SD cross section in the left branch solution, the neutralino should be heavier than about 300 GeV in order to satisfy the WMAP data. As was mentioned, the exclusion by CDMSII bounds depends on the strange contents in the nucleon, f_s. If f_s is a larger value, the left branch solution for heavier neutralino
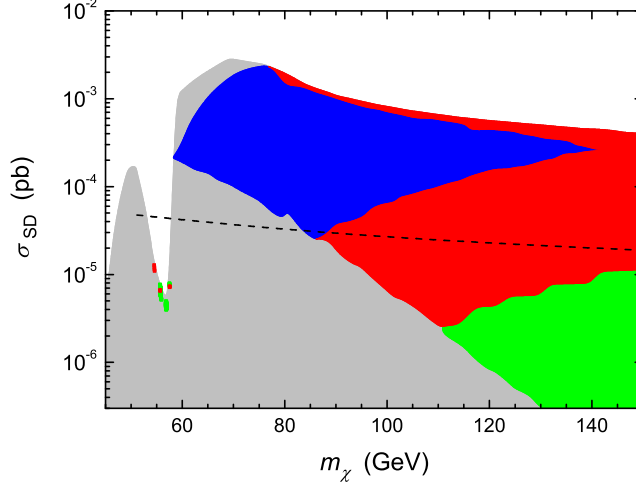
9

Figure 3: SD cross section vs neutralino mass for $\Omega h^2 = 0.11$, $\tan\beta = 40$, $m_0 = 2$ TeV, $A_0 = 0$. We choose $f_s = 0.03$. The green region satisfies sparticle mass bounds, the Br$(b \to s\gamma)$ and m_h bounds and is allowed by CDMSII and XENON100. The red region is the subset of the green region for which $\sigma_{\rm SI} > 10^{-8}$ pb. The blue region is excluded by the CDMSII and XENON100 bounds. For 80 GeV $\lesssim m_{\tilde\chi_1} \lesssim 130$ GeV, the region just below the maximal SD cross section is excluded (depending on f_s). The dashed line indicates the expected sensitivity of IceCube-80/Deep Core (1800d) [17].

can be already excluded.

We note that Br$(B_s \to \mu^+\mu^-)$ can be large and comparable to the current bound (even if $\tan\beta = 30$) when μ is large, of order ~ 2 TeV (A-funnel solution). This is because of the finite correction from gluino loop contribution, which generates a b-s flavor changing Higgs coupling. Although the gluino FCNC is suppressed, the contribution can be large, for large μ, due to the large left-right sbottom mixing. The cross sections are certainly small for the large μ solution. The corresponding points can be seen in the case of $m_{\chi_1} = 150$ GeV at the bottom-right side in Fig. 2 (left panel).

We should mention that the left branch solution is disfavored especially if $m_{\tilde\chi_1}$ is small and $\tan\beta$ is large, since the charged Higgs mass (more precisely, $m_{H^+}^2/\tan\beta$) is bounded by the $B \to \tau\bar\nu$ and $D \to \tau\bar\nu$ constraints [40, 41]. However, the bounds are sensitive to the quark mixing parameters, and so we keep the left branch solution for the WMAP relic density. The SD cross section is not sensitive to $\tan\beta$ (if $\tan\beta \gtrsim 20$), and thus there is a possibility to observe a large Br$(B_s \to \mu^+\mu^-)$ at LHCb and a large SD cross section at the IceCube/Deep Core, if $\tan\beta \sim 30$ and $m_{\tilde\chi_1} \gtrsim 300$ GeV.

Since m_A can be small in the left branch, the bound from direct detection can exclude the

blue points in Fig. 2. If $m_{\tilde{\chi}_1}$ is small ($\lesssim 100$ GeV), a region from the right branch of the WMAP solution can even be excluded.

In Fig. 3, we plot the correlation between the SD cross section and the neutralino mass in the right branch solution for $\Omega h^2 = 0.11$. We find that a region just below the maximal values of the possible SD cross section is excluded by the CDMSII experiment, for 80 GeV $\lesssim m_{\tilde{\chi}_1} \lesssim 130$ GeV. Along the WMAP solution for the right branch (shown in Fig. 1), the SI cross section increases for smaller μ values. However, since m_A is larger in this direction, the SI cross section becomes maximal and then decreases after that, while μ asymptotes to a minimum. As a result, the region just below the maximal SD cross section is excluded if the maximal value of the SI cross section is larger than the CDMSII bound.

From Fig. 3 one can see that $m_{\tilde{\chi}_1} \lesssim 80$ GeV is excluded. The exact numerical value depends on the chosen f_s value. For example, if $f_s = 0.118$ (ISAJET default) is used, the maximal SD cross section is excluded for $m_{\tilde{\chi}_1} \lesssim 120$ GeV.

5   LHC phenomenology

As previously mentioned, the bino-Higgsino mixing needs to be well-tempered, especially if $m_A \gg 2m_{\tilde{\chi}_1}$ and sfermions are heavy. In this case, since the bino and Higgsino masses M_1 and μ need to be close together, the three eigenvalues of the neutralino mass matrix are approximately degenerate:

$$m_{\tilde{\chi}_2} - m_{\tilde{\chi}_1}, \ m_{\tilde{\chi}_3} - m_{\tilde{\chi}_1} < M_Z. \tag{4}$$

The second and third lightest neutralinos ($\tilde{\chi}_2, \tilde{\chi}_3$), produced from the decays of squarks and/or gluino, themselves decay into $\tilde{\chi}_1 \ell^+ \ell^-$. The end points of the dilepton invariant mass, $M_{\ell\ell}$, gives the mass differences of the neutralinos [42]. If the mass differences are less than about 80 GeV, we can measure two end points of the $M_{\ell\ell}$ distribution, and this can yield important information about the neutralino mass parameters. In order to measure the mass differences, the end points should be a little less than the Z boson mass in order to avoid a Z-pole of the distribution.

The neutralino mass matrix is commonly written as

$$M_\chi = \begin{pmatrix} M_1 & 0 & -M_Z \cos\beta \sin\theta_W & M_Z \sin\beta \sin\theta_W \\ 0 & M_2 & M_Z \cos\beta \cos\theta_W & -M_Z \sin\beta \cos\theta_W \\ -M_Z \cos\beta \sin\theta_W & M_Z \cos\beta \cos\theta_W & 0 & -\mu \\ M_Z \sin\beta \sin\theta_W & -M_Z \sin\beta \cos\theta_W & -\mu & 0 \end{pmatrix}. \tag{5}$$

Because there are only off-diagonal entries in the Higgsino block, the second and third mass eigenvalues are of opposite signature in the case of bino-Higgsino dark matter. The relative

sign of the neutralino mass is physical for the $M_{\ell\ell}$ distribution. In the limit where $m_{\tilde{\chi}_i} \ll m_{\tilde{\ell}}$, the differential decay width of $\tilde{\chi}_i \to \tilde{\chi}_1 \ell\ell$ is [43, 44, 45]

$$
\frac{d\Gamma}{dM_{\ell\ell}} \propto \frac{M_{\ell\ell}}{(M_{\ell\ell}^2 - M_Z^2)^2} \sqrt{((m_{\tilde{\chi}_i} - m_{\tilde{\chi}_1})^2 - M_{\ell\ell}^2)((m_{\tilde{\chi}_i} + m_{\tilde{\chi}_1})^2 - M_{\ell\ell}^2)} \tag{6}
$$
$$
\times \left((\eta_i m_{\tilde{\chi}_i} - m_{\tilde{\chi}_1})^2 + 2M_{\ell\ell}^2\right)\left((\eta_i m_{\tilde{\chi}_i} + m_{\tilde{\chi}_1})^2 - M_{\ell\ell}^2\right).
$$

As a convention, all $m_{\tilde{\chi}_i}$ take positive values, and the eigenstate $\tilde{\chi}_1$ is assigned a positive mass eigenvalue. If the remaining eigenstates $\tilde{\chi}_i$, $i = 2, 3, 4$, have a positive (negative) eigenvalue, we define the corresponding $\eta_i = 1$ (-1). We use Eq. (6) even though this analysis is perhaps a bit too optimistic.

It is easy to see that in the limit where $m_{\tilde{\chi}_i} - m_{\tilde{\chi}_1} \ll M_Z$, the distribution is almost symmetric for $\eta_i = -1$, and the peak of the distribution is at half of the end point $M_{\ell\ell}^{\text{end}} = m_{\tilde{\chi}_i} - m_{\tilde{\chi}_1}$. Due to the factor $M_{\ell\ell}/(M_{\ell\ell}^2 - M_Z^2)^2$, the distribution near the end point is enhanced when the mass difference is close to M_Z. For $\eta_i = 1$, the peak shifts towards the end point even if the mass difference is not close to M_Z. Therefore, by observing the shape of the $M_{\ell\ell}$ distribution, one can distinguish between η_i positive or negative.

We denote the eigenstate where $\eta_i = 1$ (-1) as $\tilde{\chi}_p$ $(\tilde{\chi}_m)$. Then, by definition, $\tilde{\chi}_2 = \tilde{\chi}_p$ and $\tilde{\chi}_3 = \tilde{\chi}_m$ if $m_{\tilde{\chi}_p} < m_{\tilde{\chi}_m}$, for example.

We have the following four equations among the MSSM parameters and the eigenvalues:

$$
m_{\tilde{\chi}_1} + m_{\tilde{\chi}_p} - m_{\tilde{\chi}_m} + m_{\tilde{\chi}_4} = M_1 + M_2, \tag{7}
$$
$$
m_{\tilde{\chi}_1}^2 + m_{\tilde{\chi}_p}^2 + m_{\tilde{\chi}_m}^2 + m_{\tilde{\chi}_4}^2 = M_1^2 + M_2^2 + 2(\mu^2 + M_Z^2), \tag{8}
$$
$$
m_{\tilde{\chi}_1}^3 + m_{\tilde{\chi}_p}^3 - m_{\tilde{\chi}_m}^3 + m_{\tilde{\chi}_4}^3 = M_1^3 + M_2^3 + 3(M_1 \sin^2\theta_W + M_2 \cos^2\theta_W + \mu \sin 2\beta)M_Z^2, \tag{9}
$$
$$
-m_{\tilde{\chi}_1} m_{\tilde{\chi}_p} m_{\tilde{\chi}_m} m_{\tilde{\chi}_4} = -\mu^2 M_1 M_2 + \mu M_Z^2(M_1 \cos^2\theta_W + M_2 \sin^2\theta_W) \sin 2\beta. \tag{10}
$$

Suppose that the mass differences, $D_p \equiv m_{\tilde{\chi}_p} - m_{\tilde{\chi}_1}$ and $D_m \equiv m_{\tilde{\chi}_m} - m_{\tilde{\chi}_1}$, are accurately measured at the LHC (which can be done to an accuracy of ± 1 GeV [46]), and there remain six unknown parameters: $m_{\tilde{\chi}_1}$, $m_{\tilde{\chi}_4}$, M_1, M_2, μ and $\tan\beta$. If gaugino unification is assumed, the ratio M_2/M_1 is almost fixed at low energy in the neutralino mass matrix. We can then solve the equation as a function of $\tan\beta$.

Assuming that D_p and D_m are measured to be 60 GeV and 80 GeV respectively at the LHC, we plot the solution for M_1 as a function of $\tan\beta$ in Fig. 4. The solution is less sensitive to $\tan\beta$ if $\tan\beta \gtrsim 20$, which is reasonable from the form of the neutralino mass matrix and the fact that when $M_1 \sim \mu$, $M_Z^2 \sin 2\beta$ can be neglected in the equations for large $\tan\beta$. To solve the equations, we assume that the μ parameter is real.

If squarks are much heavier than the gluino (as in the focus point/hyperbolic branch solution in the constrained MSSM (CMSSM) [47]), the gluino mass can be measured (to within an
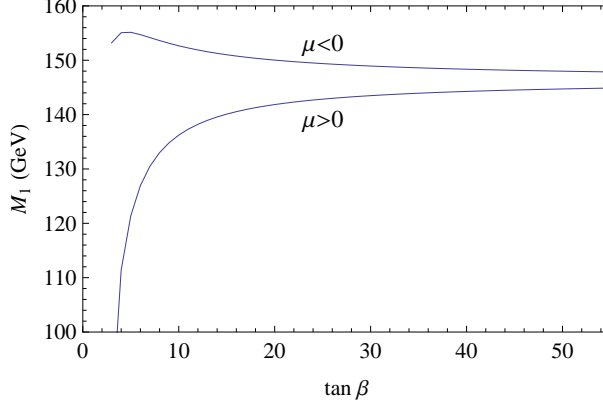
12

Figure 4: Plot of M_1 vs. $\tan\beta$ for $D_p = m_{\tilde{\chi}_p} - m_{\tilde{\chi}_1} = 60$ GeV and $D_m = m_{\tilde{\chi}_m} - m_{\tilde{\chi}_1} = 80$ GeV. Gaugino mass unification is assumed, $M_2/M_1 \simeq 2$.

accuracy of 10%) [48]. We can then determine whether or not we have gaugino mass unification for M_1 and M_3. In the example of Fig. 4, if M_3 is measured to be about 900 GeV, we may conclude that there exists nice unification of gaugino masses (M_1 and M_3) for $\tan\beta \gtrsim 20$. If M_3 is less than about 900 GeV, unification is still possible for $\tan\beta \lesssim 10$.

A model-independent measurement of $\tan\beta$ is important to conclude whether we have gaugino mass unification from the measurement of neutralino mass differences. It is hard to determine $\tan\beta$ at the LHC model-independently, but it can be measured by a future $e^+ e^-$ linear collider [49].

As previously mentioned, for large $\tan\beta$ the solution for M_1 (as shown in Fig. 4) becomes less sensitive to $\tan\beta$. In this case, m_{χ_1} can also be restricted from the measurement of the dilepton invariant mass distribution. The SI cross section is large, $\sim 10^{-8}$ pb, for the well-tempered bino-Higgsino LSP, and thus it can be expected that $m_{\tilde{\chi}_1}$ is measured by the distribution of recoil energy in direct detection experiments. If the LSP mass is accurately measured, we can determine whether $\tan\beta$ is small ($\lesssim 10$) or not, by comparing the restriction from the measurements of neutralino mass differences. To do this, however, we need to assume gaugino mass unification for M_1 and M_2.

In Fig. 5, we plot the lightest neutralino mass $m_{\tilde{\chi}_1}$ as a function of the ratio M_2/M_1, with $\tan\beta = 30$, $D_p = 60$ GeV and $D_m = 80$ GeV. If it turns out that $m_{\tilde{\chi}_1}$ is larger than about 140 GeV from the direct detection experiments, the ratio M_2/M_1 needs to be smaller than 2 ($M_2/M_1 \simeq 2$ is the expectation from gaugino mass unification). In this case, bino-wino-Higgsino tri-mixing may be realized. If $m_{\tilde{\chi}_1}$ is less than 140 GeV, it is possible that either M_2/M_1 is larger than 2 or gaugino unification is realized for $\tan\beta \lesssim 10$. Once one knows that $\tan\beta$ is large ($\gtrsim 20$) from other experiments such as $\mathrm{Br}(B_s \to \mu^+\mu^-)$, for instance, one can
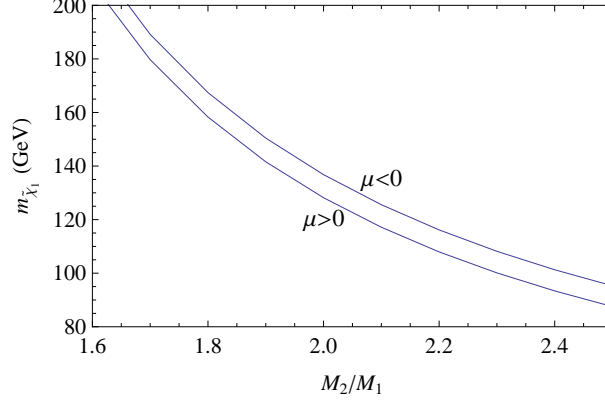
13

Figure 5: The lightest neutralino mass $m_{\tilde{\chi}_1}$ is plotted as a function of the gaugino mass ratio M_2/M_1 for $\tan\beta = 30$, $D_p = 60$, and $D_m = 80$ GeV.

conclude that M_2/M_1 is larger than 2. Therefore, an independent measurement of $\tan\beta$ will be important in order to test gaugino unification from the D_p and D_m measurements.

In Fig. 6, we plot the solutions of Eqs.(7)-(10) for $D_p, D_m < 100$ GeV, assuming $\tan\beta = 30$, $\mu > 0$ and gaugino mass unification, $M_2/M_1 \simeq 2$. In the black region, there are solutions for given D_p, D_m, but the chargino mass bound, $m_{\tilde{\chi}_1^+} > 103$ GeV, is not satisfied. The colored regions blue, light and dark green, satisfy the chargino mass bound.

The $M_{\ell\ell}$ distribution, of course, is independent of whether the WMAP relic density is provided for or not. We present different color codings for varying WMAP relic density in the case where sfermion and heavier Higgs masses are 2 TeV to make the bino-Higgsino mixing well-tempered. We show $\Omega h^2 < 0.085$ in blue, $0.085 < \Omega h^2 < 0.13$ in light green, and $\Omega h^2 > 0.13$ in dark green color. The focus point/hyperbolic branch solutions in the CMSSM should lie in the light green region. However, if $\tan\beta \sim 50$, the heavier Higgs can be light which enhances the neutralino annihilation cross section. As a result, the focus point/hyperbolic branch of the CMSSM will penetrate into the dark green region of Fig. 6. It is not necessary to have the unification condition for SUSY breaking scalar masses since the neutralino mass differences are independent of this assumption. If coannihilation with a sfermion is present, the relic density is reduced and the dark green region can satisfy the WMAP data.

The reason that the shape of WMAP solutions resembles a heart is as follows: For the left ventricle, the lightest neutralino mass is less than about 170 GeV. (Therefore, the SD cross section is larger for the left side, $D_p \simeq 45 - 60$ GeV). For the right ventricle, $\tilde{\chi}_1$ is heavier than 170 GeV, and so the neutralinos can pair-annihilate to a top pair, and thus smaller bino-Higgsino mixing is needed, and D_m becomes larger. In bino-Higgsino dark matter, a larger Higgsino component is required for a heavier neutralino in the absence of coannihilations with scalar particles. So the heavier the neutralino, the closer μ needs to be to M_1. Therefore, D_m
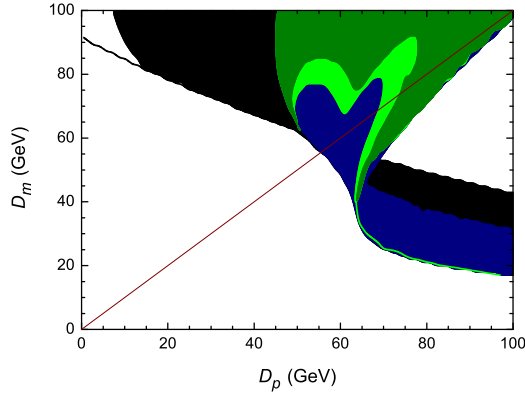
14

Figure 6: Map of the solution for given mass differences, D_p, D_m in the case where gaugino mass is unified, $M_2/M_1 \simeq 2$. The black colored region is excluded by the chargino mass bound. The other color codes correspond to varying relic density Ωh^2, as explained in the text.

and D_p decrease for larger m_{χ_1} ($\gtrsim 200$ GeV), which forms the right ventricle. For $m_{\tilde{\chi}_1} \gtrsim 300$ GeV, the ordering of mass eigenvalues of $\tilde{\chi}_p$ and $\tilde{\chi}_m$ is flipped since μ is closer to M_1, namely $D_m < D_p$ for $m_{\tilde{\chi}_1} \gtrsim 300$ GeV. The light green line for $D_m < 40$ GeV corresponds to a Higgsino-like LSP ($\mu < M_1$), with $m_{\tilde{\chi}_1} \sim 1$ TeV.

Except for $m_{\tilde{\chi}_1} \sim 200$ GeV, the SI cross section can be 10^{-8} pb even if $m_A = 2$ TeV. In the case of $m_{\tilde{\chi}_1} \sim 200$ GeV, D_m is close to M_Z to satisfy the neutralino relic density. It may then be difficult to measure it due to the Z-pole of the $M_{\ell\ell}$ distribution. For $\tan\beta \lesssim 10$, D_m may be larger and closer to M_Z for the WMAP solution, even for $m_{\tilde{\chi}_1} \sim 100$ GeV. The SD and SI cross sections can be large even in this case. If the cross sections are experimentally observed, the LSP is bino-Higgsino dark matter and one of the mass differences can restrict the parameter space.

It is interesting that $D_p < D_m$ is satisfied for not too heavy LSP ($m_{\tilde{\chi}_1} \lesssim 300$ GeV), while for a relatively heavy LSP, the opposite holds, $D_m < D_p$. This just follows from the neutralino mass matrix when M_1 and M_2 have the same sign for the well-tempered bino-Higgsino dark matter. If M_1 and M_2 have opposite signs, on the other hand, $D_m < D_p$ as long as the chargino mass bound is satisfied and $D_p < 100$ GeV. In Fig. 7, we plot the solutions for $M_2 = -2M_1$ and $\tan\beta = 30$.

Because the $M_{\ell\ell}$ distribution looks very different, it is a powerful tool to observe the relative signatures of M_1 and M_2 if the lightest neutralino is not heavy, $m_{\tilde{\chi}_1} \lesssim 300$ GeV. If $M_1 M_2 > 0$ for the relatively light LSP, $D_p < D_m$ is satisfied. The distribution near the end point is then enhanced, and it has a sharp edge near $M_{\ell\ell} \sim D_p$. If the edge is not enhanced and it turns out
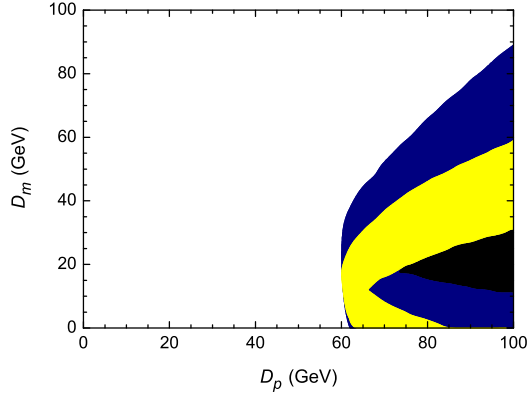
Figure 7: Map of the solutions for given mass differences in the case of $M_2/M_1 = -2$. Black region is excluded by the chargino mass bound. Yellow region satisfies $\sigma_{\rm SD} > 10^{-4}$ pb. It is important that there is no point for $D_m > D_p$, which means that the eigenvalues of $\tilde{\chi}_1$ and $\tilde{\chi}_2$ have opposite signs.

that the LSP is light, it follows that $M_1 M_2 < 0$ and gaugino mass unification is not realized.

We note that the edge can be enhanced even if $D_m < D_p$ is satisfied for $M_1 M_2 < 0$ due to the factor $M_{\ell\ell}/(M_{\ell\ell}^2 - M_Z^2)^2$ in the distribution function. This can happen when D_m is close to M_Z, which is not the case for the light neutralino. For example, in Fig. 7 we show the region where the SD cross section is more than 10^{-4} pb. The region corresponds to a light neutralino, and D_p is less than 50 GeV. In this case, the edge of the distribution cannot be enhanced.

Finally, it is also possible for $\tilde{\chi}_2$ and $\tilde{\chi}_3$ to have mass eigenvalues with the same signature if $|M_2/M_1| \sim 1$.

6   Summary

We have investigated the direct and indirect detection of the bino-Higgsino dark matter scenario, and explored its implications for the LHC. We first presented the prediction of SD cross section and the branching ratio of $B_s \to \mu^+\mu^-$, assuming that the WMAP relic density constraint is satisfied. Because the relic density restricts the bino-Higgsino mixing, the SD cross section is predicted for given m_A. For the WMAP compatible solution, we have two regions for bino-Higgsino dark matter : (1) $m_A < 2m_{\tilde{\chi}_1}$, (2) $m_A > 2m_{\tilde{\chi}_1}$. Since pair annihilation channels can open up in region (1), the bino-Higgsino mixing here should be smaller than in region (2). In region (1), the SD cross section is therefore smaller, and the neutralino should be sufficiently heavy for the SD cross section to be observed. We find that the SD cross section can be observed indirectly by the neutrino flux from the sun if $m_{\tilde{\chi}_1} \gtrsim 300$ GeV. In region (1), the branching

ratio for $B_s \rightarrow \mu^+\mu^-$ can be enhanced, and $\mathrm{Br}(b \rightarrow s\gamma)$ constraint gives a lower bound in flavor universal models which can be tested at LHCb. The CDMSII bound can exclude a large branching ratio of $B_s \rightarrow \mu^+\mu^-$. In region (2), on the other hand, the bino-Higgsino mixing is well-tempered and the SD cross section is large enough to be observed. For a neutralino mass less than about 100 GeV, the CDMSII bound constrains the SD cross section even in region (2). A SD cross section just below the maximal value, for given neutralino mass, is excluded by the CDMSII experiment. This exclusion depends on the strange sea-quark content f_s in the nucleon (multiplied by the strange mass). If the maximal SD cross section for $m_{\tilde{\chi}_1} \simeq 80 - 100$ GeV is observed, a smaller value ($f_s \sim 0.03$) consistent with the recent results from lattice calculations will be preferred.

We next studied the LHC phenomenology of bino-Higgsino dark matter. Because the mass differences of the neutralinos in the case of well-tempered bino-Higgsino dark matter are small, they can be measured by the dilepton invariant mass distribution. From the neutralino mass differences, we may be able to infer whether gaugino masses are unified or not. For this, it turns out that $\tan\beta$ is an important parameter. If we find that $\tan\beta$ is large, say from an observation such as $\mathrm{Br}(B_s \rightarrow \mu^+\mu^-)$, the gaugino mass ratio at the weak scale can be obtained from the mass differences. The shape of the dilepton invariant mass distribution depends on the relative signatures of the neutralino mass eigenvalues. This distribution will be a powerful tool in providing important information about neutralino masses and the relative signatures of the gaugino masses.

If gaugino mass unification is assumed and two of the mass differences of the neutralinos are measured, $\tan\beta$ can be determined, and the bino-Higgsino dark matter relic abundance is then reproduced. The relic density thus deduced from collider measurements provides a strong hint for identifying the nature of dark matter if it coincides with the WMAP data. If the two do not coincide, we cannot decide whether gaugino unification is not satisfied or the neutralino LSP alone does not saturate the WMAP measured relic abundance. A model-independent measurement of $\tan\beta$ provides a strong hint to solve this dilemma. In general, it is hard to measure $\tan\beta$ model-independently at the LHC, but it is possible at a future linear collider. The polarization of τ lepton may give us a hint of the size of $\tan\beta$ if sleptons are light enough in the bino-Higgsino dark matter scenario [50]. We have in this paper assumed that all the sfermions are heavy in order to make their mass parameters insensitive to our discussion, but this assumption can be relaxed. The large bino-Higgsino mixing can provide various features for collider phenomenology, such as τ polarization, if on-shell sleptons appear in the cascade decays.

From a theoretical point of view, a confirmation of the bino-Higgsino dark matter scenario

can provide important impetus to investigations of SUSY breaking. A bino-Higgsino dark matter needs a relatively small Higgsino mass μ. In fact, small μ is preferable if it is a parameter independent of the SUSY breaking scale, while μ can be large among the electroweak symmetry breaking vacua if it depends on a single SUSY breaking scale parameter [51]. Therefore, testing the bino-Higgsino dark matter scenario can serve as an important avenue for distinguishing among the various models of SUSY breaking.

In conclusion, the lightest neutralino with an appropriate composition of bino and Higgsino components is a compelling dark matter candidate. This will soon be tested by the ongoing and planned direct detection experiments, and indirectly at the IceCube neutrino telescope through pair annihilation. A mixed bino-Higgsino dark matter particle can also lead to characteristic signals at the LHC as we have discussed.

Acknowledgments

References

[1] E. Komatsu *et al.* [WMAP Collaboration], Astrophys. J. Suppl. **180**, 330 (2009).

[2] For a review see G. Jungman, M. Kamionkowski and K. Griest, Phys. Rept. **267**, 195 (1996) and references therein.

[3] G. Bertone, D. Hooper and J. Silk, Phys. Rept. **405**, 279 (2005); G. Bertone and D. Merritt, Mod. Phys. Lett. A **20**, 1021 (2005); J. Carr, G. Lamanna and J. Lavalle, Rept. Prog. Phys. **69**, 2475 (2006).

[4] J. L. Feng, K. T. Matchev and F. Wilczek, Phys. Lett. B **482**, 388 (2000); Phys. Rev. D **63**, 045024 (2001); H. Baer, C. Balazs and A. Belyaev, JHEP **0203**, 042 (2002).

[5] G. F. Giudice and A. Romanino, Nucl. Phys. B **699**, 65 (2004) [Erratum-ibid. B **706**, 65 (2005)]; A. Pierce, Phys. Rev. D **70**, 075006 (2004); A. Masiero, S. Profumo and P. Ullio, Nucl. Phys. B **712**, 86 (2005); N. Arkani-Hamed, A. Delgado and G. F. Giudice, Nucl. Phys. B **741**, 108 (2006); H. Baer, A. Mustafayev, E. K. Park and X. Tata, JCAP **0701**, 017 (2007).

[6] Y. Mambrini and C. Munoz, Astropart. Phys. **24**, 208 (2005); H. Baer, A. Mustafayev, S. Profumo, A. Belyaev and X. Tata, JHEP **0507**, 065 (2005); H. Baer, T. Krupovnickas, S. Profumo and P. Ullio, JHEP **0510**, 020 (2005); J. Ellis, K. A. Olive and P. Sandick, New J. Phys. **11**, 105015 (2009).

[7] J. L. Feng, K. T. Matchev and T. Moroi, Phys. Rev. D **61**, 075005 (2000); Phys. Rev. Lett. **84**, 2322 (2000); J. L. Feng and F. Wilczek, Phys. Lett. B **631**, 170 (2005); U. Chattopadhyay, T. Ibrahim and D. P. Roy, Phys. Rev. D **64**, 013004 (2001); U. Chattopadhyay, A. Datta, A. Datta, A. Datta and D. P. Roy, Phys. Lett. B **493**, 127 (2000); S. P. Das, A. Datta, M. Guchait, M. Maity and S. Mukherjee, Eur. Phys. J. C **54**, 645 (2008).

[8] K. L. Chan, U. Chattopadhyay and P. Nath, Phys. Rev. D **58**, 096004 (1998); U. Chattopadhyay, A. Corsetti and P. Nath, Phys. Rev. D **68**, 035005 (2003).

[9] Z. Ahmed *et al.* [The CDMS-II Collaboration], Science **327**, 1619 (2010).

[10] Talk by J. Gascon [EDELWEISS Collaboration] at ICHEP2010 conference, Paris, France.

[11] I. Gogoladze, R. Khalid, S. Raza and Q. Shafi, Mod. Phys. Lett. A, **25**, 3371 (2010); M. Asano, S. Matsumoto, M. Senami and H. Sugiyama, JHEP **1007**, 013 (2010); M. Farina, D. Pappadopulo and A. Strumia, Phys. Lett. B **688**, 329 (2010); X. G. He, T. Li, X. Q. Li, J. Tandean and H. C. Tsai, Phys. Lett. B **688**, 332 (2010); M. Ibe and T. T. Yanagida, Phys. Rev. D **81**, 035017 (2010); M. Kadastik, K. Kannike, A. Racioppi and M. Raidal, arXiv:0912.3797 [hep-ph]; U. Chattopadhyay, D. Das, D. K. Ghosh and M. Maity, Phys. Rev. D **82**, 075013 (2010); I. Gogoladze, R. Khalid, S. Raza and Q. Shafi, arXiv:1008.2765 [hep-ph].

[12] A. Bottino, F. Donato, N. Fornengo and S. Scopel, Phys. Rev. D **81**, 107302 (2010); M. Holmes and B. D. Nelson, Phys. Rev. D **81**, 055002 (2010); K. Cheung and T. C. Yuan, Phys. Lett. B **685**, 182 (2010); J. Hisano, K. Nakayama and M. Yamanaka, Phys. Lett. B **684**, 246 (2010); D. P. Roy, Phys. Rev. D **81**, 057701 (2010); R. Allahverdi, B. Dutta and Y. Santoso, Phys. Lett. B **687**, 225 (2010); D. Feldman, Z. Liu and P. Nath, Phys. Rev. D **81**, 095009 (2010); J. Cao, K. i. Hikasa, W. Wang, J. M. Yang and L. X. Yu, JHEP **1007**, 044 (2010); Phys. Rev. D **82**, 051701 (2010); D. Feldman, Z. Liu, P. Nath and G. Peim, Phys. Rev. D **81**, 095017 (2010); D. Feldman, Z. Liu and P. Nath, Phys. Rev. D **81**, 117701 (2010).

[13] E. Aprile [XENON100 Collaboration], AIP Conf. Proc. **1166**, 205 (2009); Phys. Rev. Lett. **105**, 131302 (2010).

[14] R. W. Schnee *et al.* [The SuperCDMS Collaboration], arXiv:astro-ph/0502435.

[15] K. Abe [XMASS Collaboration], AIP Conf. Proc. **1182**, 268 (2009).

[16] M. Ackermann *et al.* [AMANDA Collaboration], Astropart. Phys. **24**, 459 (2006).

[17] K. Hultqvist, IceCube collaboration, arXiv:1003.2300 [astro-ph.HE].

[18] T. Cohen, D. J. Phalen and A. Pierce, Phys. Rev. D **81**, 116001 (2010).

[19] S. R. Choudhury and N. Gaur, Phys. Lett. B **451**, 86 (1999); K. S. Babu and C. F. Kolda, Phys. Rev. Lett. **84**, 228 (2000).

[20] CDF collaboration, CDF Public Note 9892.

[21] M. Lenzi, arXiv:0710.5056 [hep-ex]; M. O. Bettler [LHCb Collaboration], arXiv:0910.0942 [hep-ex].

[22] J. L. Feng and M. E. Peskin, Phys. Rev. D **64**, 115002 (2001).

[23] N. Arkani-Hamed, G. L. Kane, J. Thaler and L. T. Wang, JHEP **0608**, 070 (2006).

[24] G. Polesello and D. R. Tovey, JHEP **0405**, 071 (2004); M. M. Nojiri, G. Polesello and D. R. Tovey, JHEP **0603**, 063 (2006); S. G. Kim, N. Maekawa, K. I. Nagao, M. M. Nojiri and K. Sakurai, JHEP **0910**, 005 (2009).

[25] R. L. Arnowitt, B. Dutta, T. Kamon, N. Kolev and D. A. Toback, Phys. Lett. B **639**, 46 (2006); R. L. Arnowitt *et al.*, Phys. Lett. B **649**, 73 (2007); R. L. Arnowitt, B. Dutta, A. Gurrola, T. Kamon, A. Krislock and D. Toback, Phys. Rev. Lett. **100**, 231802 (2008).

[26] P. Nath *et al.*, Nucl. Phys. Proc. Suppl. **200-202**, 185 (2010); B. Dutta, Talk at BSM-SUSY-09 and PASCOS-09.

[27] B. Dutta, T. Kamon, A. Krislock, N. Kolev and Y. Oh, arXiv:1008.3380 [hep-ph].

[28] B. Altunkaynak, P. Grajek, M. Holmes, G. Kane and B. D. Nelson, JHEP **0904**, 114 (2009).

[29] H. Baer and M. Brhlik, Phys. Rev. D **57**, 567 (1998).

[30] J. Ellis, K. A. Olive and P. Sandick, New J. Phys. **11**, 105015 (2009); D. Das, A. Goudelis and Y. Mambrini, JCAP **1012**, 018 (2010).

[31] H. Ohki *et al.*, Phys. Rev. D **78**, 054502 (2008); arXiv:0910.3271 [hep-lat]; K. Takeda, S. Aoki, S. Hashimoto, T. Kaneko, T. Onogi and N. Yamada [JLQCD collaboration], arXiv:0910.5036 [hep-lat].

[32] R. D. Young and A. W. Thomas, Phys. Rev. D **81**, 014503 (2010); Nucl. Phys. A **844**, 266C (2010).

[33] D. Toussaint and W. Freeman [MILC Collaboration], Phys. Rev. Lett. **103**, 122002 (2009).

[34] H. Baer, F. E. Paige, S. D. Protopopescu and X. Tata, arXiv:hep-ph/0001086.

[35] K. Nakamura [Particle Data Group], J. Phys. G **37**, 075021 (2010).

[36] M. Drees and M. M. Nojiri, Phys. Rev. D **47**, 376 (1993); P. Nath and R. L. Arnowitt, Phys. Rev. Lett. **70**, 3696 (1993); H. Baer and M. Brhlik, Phys. Rev. D **53**, 597 (1996); H. Baer, M. Brhlik, M. A. Diaz, J. Ferrandis, P. Mercadante, P. Quintana and X. Tata, Phys. Rev. D **63**, 015007 (2000); J. R. Ellis, T. Falk, G. Ganis, K. A. Olive and M. Srednicki, Phys. Lett. B **510**, 236 (2001); A. B. Lahanas and V. C. Spanos, Eur. Phys. J. C **23**, 185 (2002).

[37] J. Ellis, K. A. Olive, C. Savage and V. C. Spanos, Phys. Rev. D **81**, 085004 (2010).

[38] J. R. Ellis, K. A. Olive, Y. Santoso and V. C. Spanos, JHEP **0605**, 063 (2006).

[39] B. Dutta and Y. Mimura, Phys. Lett. B **677**, 164 (2009); B. Dutta, Y. Mimura and Y. Santoso, Phys. Rev. D **80**, 095005 (2009); Phys. Rev. D **82**, 055017 (2010).

[40] W. S. Hou, Phys. Rev. D **48**, 2342 (1993); M. Bona *et al.* [UTfit Collaboration], Phys. Lett. B **687**, 61 (2010).

[41] A. G. Akeroyd and F. Mahmoudi, JHEP **0904**, 121 (2009).

[42] H. Baer, K. Hagiwara and X. Tata, Phys. Rev. D **35**, 1598 (1987).

[43] M. M. Nojiri and Y. Yamada, Phys. Rev. D **60**, 015006 (1999).

[44] R. Kitano and Y. Nomura, Phys. Rev. D **73**, 095004 (2006).

[45] U. De Sanctis, T. Lari, S. Montesano and C. Troncon, Eur. Phys. J. C **52**, 743 (2007).

[46] D. Tovey, Talk at PPC07; G. Moortgat-Pick, Talk at SUSY07.

[47] For recent discussions and additional references see L. Roszkowski, R. Ruiz de Austri and R. Trotta, JHEP **0707** (2007) 075; A. Belyaev, S. Dar, I. Gogoladze, A. Mustafayev and Q. Shafi, arXiv:0712.1049 [hep-ph]. D. Feldman, Z. Liu and P. Nath, JHEP **0804**, 054 (2008); J. R. Ellis, K. A. Olive and P. Sandick, JHEP **0808**, 013 (2008); F. Feroz, B. C. Allanach, M. Hobson, S. S. AbdusSalam, R. Trotta and A. M. Weber, JHEP **0810**, 064 (2008); G. Barenboim, P. Paradisi, O. Vives, E. Lunghi and W. Porod, JHEP **0804**, 079 (2008); I. Gogoladze, R. Khalid, Q. Shafi and H. Yuksel, Phys. Rev. D **79**, 055019 (2009); J. L. Kneur and N. Sahoury, Phys. Rev. D **79**, 075010 (2009); H. Baer and X. Tata, arXiv:0805.1905 [hep-ph].

[48] H. Baer, V. Barger, G. Shaughnessy, H. Summy and L. t. Wang, Phys. Rev. D **75**, 095010 (2007).

[49] M. Berggren, R. Keranen and A. Sopczak, Eur. Phys. J. direct C **2**, 8 (2000); A. Datta, A. Djouadi and J. L. Kneur, Phys. Lett. B **509**, 299 (2001).

[50] M. M. Nojiri, Phys. Rev. D **51**, 6281 (1995); A. Bartl, H. Eberl, S. Kraml, W. Majerotto and W. Porod, Z. Phys. C **73**, 469 (1997); R. M. Godbole, M. Guchait and D. P. Roy, Phys. Lett. B **618**, 193 (2005); Phys. Rev. D **79**, 095015 (2009).

[51] G. F. Giudice and R. Rattazzi, Nucl. Phys. B **757**, 19 (2006); B. Dutta and Y. Mimura, Phys. Lett. B **648**, 357 (2007).